Neural-Network Potential for the Water Molecule

Cillian Vickers-Hayes

Introduction

Machine learning offers a powerful, cost-effective alternative to repeatedly performing expensive quantum-mechanical calculations when mapping molecular potential-energy surfaces. In this project, I explore how a simple feed-forward neural network can accurately learn the H_2O potential from the provided dataset by training on one set of geometries and testing on another. Specifically, I compared two versions of the same dataset of O–H bond lengths and H–O–H angles. One unrotated set in which every molecule shares the same spatial orientation, and a rotated set in which each configuration is randomly oriented. Because true molecular energy depends only on internal geometry and not on orientation, a robust model should perform equally well on both, so I evaluated performance across all four train/test splits (unrotated→unrotated, rotated→rotated, unrotated→rotated, rotated→unrotated). Finally, I check the learned potential by comparing 1D bond-length and angle scans and by mapping a 2D potential-energy surface, demonstrating that even this minimal 64–32–1 network captures the energy landscape of water.

Methods

First the provided data was parsed, for each three-atom configuration we extract the two O–H bond lengths $r1$ and $r2$ and the H–O–H bond angle θ. This gives us a rotation and translation invariant set of vectors, allowing the network to focus purely on learning the mapping from geometry to energy.

The neural network was implemented in Keras as a simple feed-forward model with two layers of 64 and 32 neurons, each using a rectified linear unit, activation, and a single linear output neuron that predicts the energy. The random seed was fixed to ensure reproducibility for the results. Before training the inputs were standardize as to have zero mean and unit variance, this helps with convergence and prevents any one feature from dominating the learning process.

An Adam optimizer was used for training, minimizing mean-squared error MSE over 200 epochs using a batch size of 32. The data set was split randomly into training and validation subsets with a 80/20 ratio. Four experiments were used to verify that the model does indeed learn the internal geometry–energy relationship rather than some orientation specific artifact. Training was performed on both the unrotated and rotated datasets, and each trained model was tested against both the unrotated and rotated data. The accuracy of the model was quantified in terms of mean-absolute error MAE, in Hartree and MSE in Hartree^2.

Lastly the same 64–32–1 network architecture was retrained on the entire unrotated dataset of all 1750 geometries, before producing the final energy landscape plots.

Results

Figure 1 shows the learning curves for the final model trained on the unrotated dataset. Rapid early convergence is evident for both curves as they drop sharply over the first roughly 60 epochs. The curves begin to plateau around 100 epochs and reach a stable value by 200 epochs with some minor late-epoch oscillations. The validation loss closely follows the training loss with no significant divergence, which indicates minimal overfitting. The final MSE values are low. This is a example of the typical learning behavior I observed for all four train/test splits. 200 epochs might have been slight overkill and 100 epochs could have achieved a similar result for less compute.

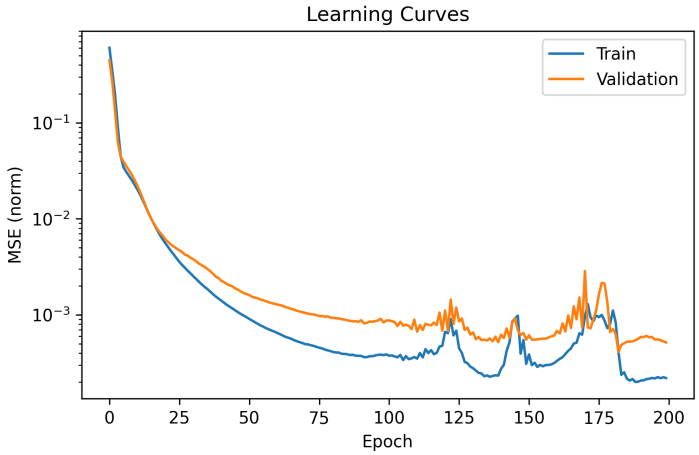

Figure 1: Training: Blue, Validation: Orange, MSE, is normalized and on a log scale over 200 epochs. This is for the final model trained on the unrotated dataset

Table 1: Mean absolute error and mean squared error both in Hartrees for each train/test combination. Values are rounded to three significant figures.

Train	Test	MAE	MSE
H2O unrotated.xyz	H2O unrotated.xyz	0.000 106	2.01×10^{-8}
H2O rotated.xyz	H2O rotated.xyz	4.12×10^{-5}	3.24×10^{-9}
H2O unrotated.xyz	H2O rotated.xyz	6.49×10^{-5}	8.60×10^{-9}
H2O rotated.xyz	H2O unrotated.xyz	6.15×10^{-5}	6.71×10^{-9}

Table 1 summarizes the errors for each train/test split performed. All models obtained very high accuracy with MAEs on the order of 10^{-4} to 10^{-5} Eh. The rotated→rotated data model performed best with the lowest error in both MAE and MSE, while the unrotated→unrotated data model performed the worst with the highest error in both measures. The cross-dataset evaluations, that is, unrotated→rotated and rotated→unrotated, produced errors in the intermediate range. This could be due to the transformation between rotated and unrotated configurations introducing subtle artifacts or inconsistencies, which may affect the model's ability to generalize cleanly across datasets. However, the difference in the error is small, which implies the models generalized to unseen orientations effectively. This confirms that using a rotation- and translation-invariant set of vectors helped make the model orientation independent. The slight advantage for the rotated→rotated model is most likely due to it offering the best diversity of data, while the unrotated→unrotated could lead the model to learn orientation artifacts rather than the geometry–energy mapping we are looking for.

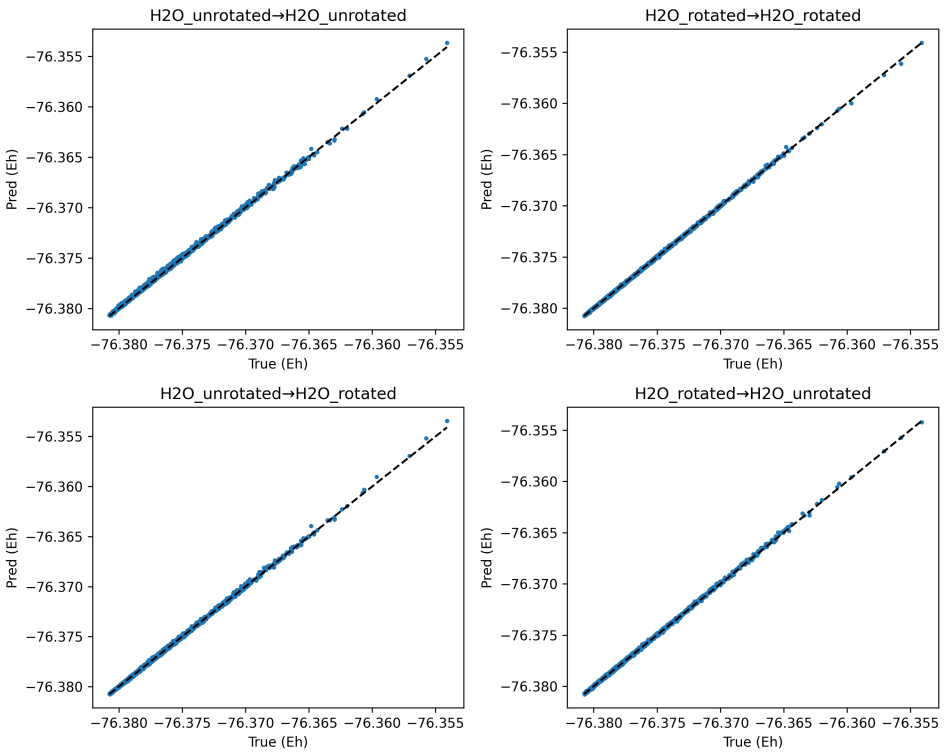

Figure 2: Parity between true and predicted energies for all four train/test splits.

For each plot in the 2×2 parity grid in Figure 2, the points are tightly clustered on the $y = x$ diagonal line, showing excellent agreement with minimal bias. As expected from Table 1, the rotated→rotated model is the most tightly packed, while the cross-dataset cases show slightly more scatter and the unrotated→unrotated model has the greatest spread. Ultimately, these plots visually confirm each model's near ideal accuracy across the full energy range.

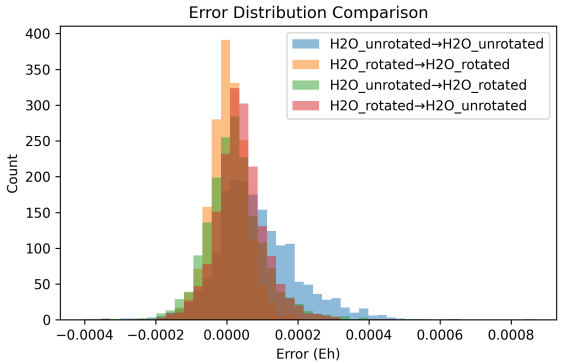

(a) Overlayed error histograms for all splits.

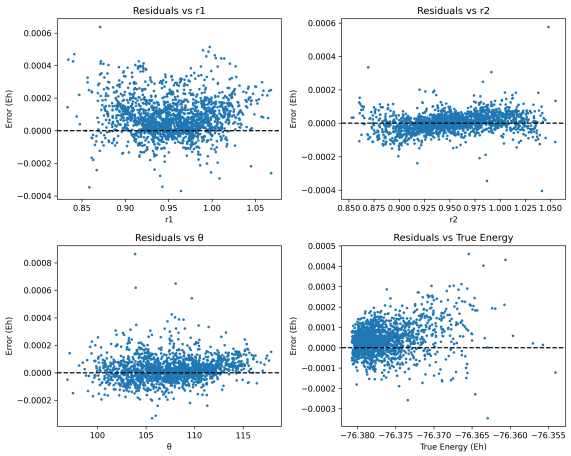

(b) Residuals for each of the four train/test splits;
(i) unrotated→unrotated vs. r_1,
(ii) rotated→rotated vs. r_2,
(iii) unrotated→rotated vs. θ,
(iv) rotated→unrotated vs. true energy.

Figure 3: Error-analysis diagnostics across all models.

The error histograms in Fig.3a and the residuals grid in Fig.3b show that the majority of prediction errors are tightly packed within $\pm 2 \times 10^{-4}$Eh for all models. The rotated–rotated model is the most tightly centered, while the unrotated–unrotated model is the most spread out. In all cases, however, the distributions are still quite narrow, and the residual plots confirm this behavior. The residuals show a slight broadening near equilibrium angles of 105–110° and at extremes such as high energy, stretched bonds, or acute/wide angles. So the model's prediction errors aren't perfectly uniform across all bond lengths and angles. This is due to these regions corresponding to parts of the true PES that are steeper, leading to higher variance in the errors. However, even these edge-case errors remain on the order of 10^{-4}, Eh with no consistent positive or negative bias. This confirms that the model is accurate for the entire range of geometries in the data, with only minor increases in errors at the far edges of the training domain.

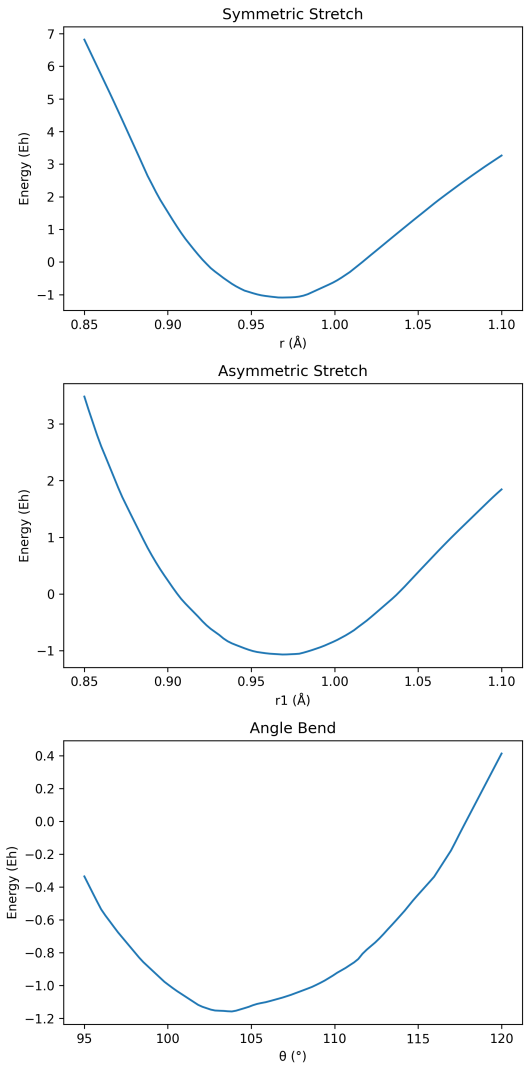

(a) Combined 1D scans

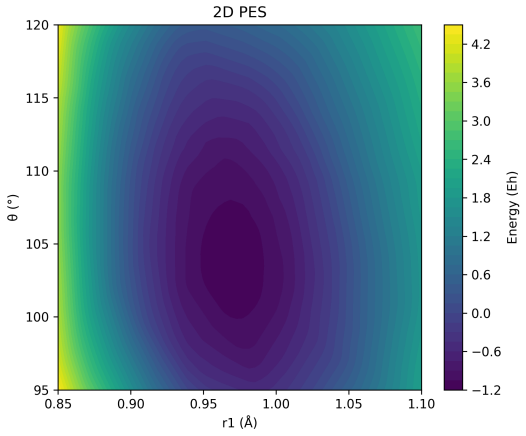

(b) 2D potential-energy surface

Figure 4: Physical validation of the final model trained on unrotated data.

This model was chosen as it had the highest errors rates and it would show us the worst case performance despite that, the model reproduces physically meaningful potential energy plots. Fig. 4a, consists of 1D energy plots for. lengthening both O–H bonds together (symmetric stretch), lengthening one O–H bond while the other remains at equilibrium length (asymmetric), and varying θ while keeping both bonds at equilibrium (angle bend). Each plot exhibit a single minimum at the equilibrium around $r_1 = r_2 \approx 0.96\,\text{Å}$, $\theta \approx 104.5°$ and have a smooth parabolic shape. This matches chemical expectations that any deviation from equilibrium increases energy. Fig. 4b, is a contour plot of the predicted energy as a function of one bond length r_1 and the angle θ, with the other bond fixed at equilibrium. There is a clear valley present at the equilibrium with energy rising as r_1 varies, also as θ moves away from $\sim 104.5°$, there is also an increase however much more slight. In the end the model forms a smooth physically plausible surface. This implies that the 64–32–1 model used even on the most error prone dataset has successfully learned a realistic H_2O potential-energy surface.

Conclusion

To conclude, it has been shown that a neural network can accurately approximate the potential energy surface of a water molecule. A 64–32–1 architecture was used with a input set of standardized rotation and translation invariant vectors. The model obtained very low prediction errors and generalized well to different orientations of the molecule. The predicted energy surface was smooth and physically reasonable and it predicted the correct equilibrium geometry and energies behavior for distortions. The main take away of this machine learning approach is the speed of the predictions once the model is, trained, and the ability to learn these complex relationships from data without explicit formulas. With this in consideration it must also be noted that the model is only reliable within its training data range and may become inaccurate outside this range. With more data in the extreme range or by incorporating physical constraints into the network, one could further improve its robustness. Extending this approach to larger molecules would require richer descriptors or deeper networks. Overall, the neural network potential for H_2O proved to be a powerful tool, illustrating how machine learning can complement traditional computational chemistry methods by providing fast and accurate energy predictions.